Photodiagnosis and Photodynamic Therapy 25 (2019) 300–308

Contents lists available at ScienceDirect

Photodiagnosis and Photodynamic Therapy

journal homepage: www.elsevier.com/locate/pdpdt

Synergistic *in vitro* effects of indocyanine green and ethylenediamine tetraacetate-mediated antimicrobial photodynamic therapy combined with antibiotics for resistant bacterial biofilms in diabetic foot infection

Xuemei Li[a], Wanting Huang[a], Xiaoying Zheng[a], Shufang Chang[b], Chengwei Liu[c], Qingfeng Cheng[d,**], Shenyin Zhu[a,*]

[a] Department of Pharmacy, First Affiliated Hospital of Chongqing Medical University, Chongqing, China
[b] Department of Obstetrics and Gynecology, Second Affiliated Hospital of Chongqing Medical University, Chongqing, China
[c] The State Key Laboratory of Infectious Diseases and Parasites, Chongqing, China
[d] Department of Endocrinology, First Affiliated Hospital of Chongqing Medical University, Chongqing, China

ARTICLE INFO

Keywords:
Photodynamic antimicrobial chemotherapy
Diabetic foot infection
Indocyanine green
EDTA
Antibacterial effect
Bacterial biofilm
Antimicrobial photodynamic therapy

ABSTRACT

Background: Antibiotic resistance has emerged as one of the most important determinants in diabetic foot infections outcomes. Antimicrobial Photodynamic therapy(A-PDT) or Photodynamic antimicrobial chemotherapy (PACT) has been proposed as an alternative approach for inactivating bacteria, especially resistant bacterial biofilms. This research investigated the synergistic effects of PACT mediated by the photosensitizer indocyanine green (ICG) and ethylenediamine tetraacetate (EDTA) combined with antibiotics against common pathogens of diabetic foot ulcer infection, including *Staphylococcus aureus* and *Pseudomonas aeruginosa*, *in vitro*.

Methods: Planktonic bacteria and biofilms of *S. aureus* and *P. aeruginosa* were incubated with ICG and EDTA, and then exposed to laser treatment. Quantitative viable counting estimates the phototoxic effects on *S. aureus* and *P. aeruginosa.* The susceptibility of methicillin-resistant *S. aureus* (MRSA) and multidrug-resistant *P. aeruginosa* (MRPA) to PACT treatment was detected by disk diffusion and micro-broth dilution methods. Confocal microscopy was used to detect the morphology of biofilms treated with PACT and antibiotics. The resazurin assay was used to quantify the metabolic activity of bacteria in biofilms.

Results: PACT mediated by ICG and EDTA led to a more pronounced antibacterial effect in *S. aureus* and *P. aeruginosa* compared with ICG alone-mediated PACT. *P. aeruginosa* was more sensitive to ICG and EDTA-mediated PACT than *S. aureus*. After PACT treatment, the susceptibility of MRSA and MRPA to antibiotics increased. Furthermore, PACT combined with antibiotic treatment significantly contributed to killing bacteria in the biofilm and disrupting biofilm structure.

Conclusions: ICG and EDTA-mediated PACT combined with antibiotics synergistically enhanced the effects of sterilization and biofilm destruction.

1. Introduction

Diabetes mellitus has become a global public health problem, and approximately 80% of diabetes patients undergo amputation of lower extremities due to foot ulcers [1]. Foot infections are one of the most important factors that leads to amputation [2]. Most diabetic foot infections (DFIs) are caused by multiple microorganisms, including aerobic Gram-positive cocci, Gram-negative bacilli, and anaerobic bacteria [3]. *Staphylococcus aureus* is the most common pathogenic microorganism, and the prevalence of methicillin-resistant *S. aureus* (MRSA) in DFI patients is 15%–30% [4]. Aerobic Gram-negative bacteria are usually co-pathogens in chronic infections, severe infections, or during antibiotic treatment [3]. Recently, the incidence of clinical multi-drug resistant organisms has increased, and 50% of isolates from DFIs show multidrug resistance [5,6]. This may prolong the duration of ulcers, increase their size 6], and increase the incidence of osteomyelitis

* Corresponding author at: Department of Pharmacy, First Affiliated Hospital of Chongqing Medical University, No. 1, Yixueyuan Road, Yuzhong District, Chongqing, 400016, China.
** Corresponding author at: Department of Endocrinology, First Affiliated Hospital of Chongqing Medical University, No. 1, Yixueyuan Road, Yuzhong District, Chongqing, 400016, China.
E-mail addresses: cqf19760516@163.com (Q. Cheng), zhushenyin0486@sina.com (S. Zhu).

https://doi.org/10.1016/j.pdpdt.2019.01.010
Received 1 November 2018; Received in revised form 28 December 2018; Accepted 7 January 2019
Available online 08 January 2019
1572-1000/

[7].

Once the underlying tissue of diabetic foot ulcers is exposed to various pathogenic bacteria, the surface of the ulcers is prone to forming biofilms [8], which are a crucial factor in persistent infections [9,10]. Biofilms, which consists of a microbial community and an extracellular polymer matrix, reduce antibiotic penetration and promote bacterial growth [11]. Minimum biofilm bactericidal concentrations are 10–1000-fold higher than those required to kill planktonic bacteria [12]. Furthermore, physiological changes (neuropathy and peripheral arterial disease) and inflammation further reduce the penetration of antimicrobial agents in diabetic foot ulcers, making it difficult for antimicrobial agents to reach target sites and achieve an effective distribution for sterilization [13], which can rapidly induce resistance. In summary, the increase in multi-drug resistant organisms, biofilm formation on the surface of infected wounds, and the poor penetration of antibiotics in DFI patients all lead to a lower efficacy of antimicrobial agents [14,15].

Photodynamic antimicrobial chemotherapy (PACT) is a non-invasive, nonspecific antimicrobial approach that does not depend on blood supply in the ulcer site, making it a promising method of eradicating pathogenic bacteria in DFIs. Furthermore, it has not been found to induce resistant strains [16] because it kills bacteria *via* cytotoxic reactive oxygen species (ROS). During PACT, a nontoxic photosensitizer is irradiated at a specific wavelength to generate a large amount of ROS (*i.e.*, singlet oxygen, superoxide anion, and oxygen radicals) to kill bacteria [17]. ROS have a tiny life span and are limited to local tissues, facilitating localized treatment without damaging surrounding tissues. The *in vitro* and *in vivo* evidence have suggested that PACT can not only stimulate growth factor production, but also reduce inflammation to promote wound healing and angiogenesis [18–20]. In some cases where chronic wounds are colonized with bacteria without infection, antibacterials are not recommended, but PACT can be used to reduce the load of colonized bacteria and promote ulcer healing. Additionally, Tardivo et al. have reported methylene blue and *O*-toluidine blue-mediated photodynamic therapy for diabetic foot osteomyelitis to prevent amputation [21]. Although the article has not explored the mechanism of photodynamic effects, it suggests that photodynamic therapy is an effective method for treating diabetic foot.

Photosensitizers that have been clinically applied to mediate PACT for chronic skin ulcers and DFIs include 5-aminolaevulinic acid (ALA), methylene blue (MB), and indocyanine green (ICG), which have absorption wavelengths of 400–630 nm [22] (ALA-induced protoporphyrin IX), 630–690 nm [23], and 600–900 nm [24], respectively; the maximum absorption wavelength of ICG is approximately 800 nm. Light penetration into tissue increases with wavelength [25], and it has been reported that penetration depth doubles from 4 mm at 500–600 nm to 8 mm at 800 nm [26]. Therefore, ICG-mediated PACT at 800 nm is more conducive to bactericidal and photobiological effects in deeper tissues. It has been reported that ICG-mediated PACT had bactericidal activity against *S. aureus*, *S. pyogenes*, *P. aeruginosa*, *E. faecalis*, *E. coli*, *Actinomycetes*, and *P. gingivalis in vitro* [27–31], and a good effect on acne and periodontitis *in vivo* [32–36]. ICG-mediated PACT has been thoroughly studied, and it is known that PACT has better phototoxic effects against Gram-positive bacteria than Gram-negative bacteria, which is due to the structure of these bacteria. The outer wall of Gram-negative bacteria consists of proteins, lipopolysaccharide trimers, and lipoproteins, which make a quasi-continuum of densely packed negative charges that prevents penetration of the anionic photosensitizer ICG into the cell; conversely, the outer wall of Gram-positive bacteria does not have such a structure [17]. Therefore, the antimicrobial effects of ICG-mediated PACT have been limited in Gram-negative bacteria.

Ethylenediamine tetraacetate (EDTA) is a metal chelating agent that is widely used in clinical therapy and preclinical research. It has been reported that EDTA chelates Mg^{2+} and Ca^{2+} from the cell wall of Gram-negative bacteria, which leads to wall instability and increases the permeability of antibiotics and photosensitizers [37–40]. Additionally, EDTA counteracts biofilms by chelating Mg^{2+} and Ca^{2+}, which maintain biofilm structure; furthermore, it also removes the iron atoms that are essential for microbial virulence and pathogenicity [39].

To date, there has not been a report about ICG and EDTA-mediated PACT alone or in combination with antibiotics for treating multi-drug resistant bacteria and their biofilms in DFIs. Thus, we investigated the effects of ICG and EDTA-mediated PACT combined with antibacterial agents on the common planktonic bacteria and their biofilms of diabetic foot infections *in vitro*. These studies will pave the way for future *in vivo* studies of ICG and EDTA-mediated PACT combined with antibacterial therapy for DFI. To the best of our knowledge, this is the first study to combine ICG and EDTA-mediated PACT with antibiotics to synergistically treat resistant bacterial biofilms in DFI.

2. Materials and methods

2.1. Bacterial strains

The microorganisms used in this study were *S. aureus* (25923; ATCC, Manassas, VA, USA), MRSA (10485), *P. aeruginosa* (27853; ATCC), and multidrug-resistant *P. aeruginosa* (MRPA) (10911). *S. aureus* (25923) and *P. aeruginosa* (27853) were gifts from the State Key Laboratory of Infectious Diseases and Parasites (Chongqing, China). The clinical isolates MRSA 10485 and MRPA 10911 were obtained from the First Affiliated Hospital of Chongqing Medical University. All strains were incubated on 5% horse blood agar plates (Jiangmen Caring Trading Company, Jiangmen, China) for 18 h at 37 °C. *S. aureus* and *P. aeruginosa* were grown aerobically in trypticase soy broth (TSB; Qingdao Haibo Biochemistry Instruments, Qingdao, China) with shaking at 37 °C for 4 h (logarithmic growth phase). Then the cells were collected by centrifugation and resuspended in phosphate-buffered saline (PBS). The optical density at 600 nm (OD_{600}) of the *S. aureus* and *P. aeruginosa* suspensions were adjusted to 0.1 and 0.05 absorbance, respectively, which represented approximately 10^7–10^8 colony forming units per milliliter (CFU/mL).

2.2. Bacterial growth

After incubating the strains in TSB overnight at 37 °C, turbidities of the bacterial suspensions were adjusted to 0.5 on the McFarland Standard with $BaSO_4$ (BIO-KONT Company, Wenzhou, China). The adjusted bacterial suspensions were diluted 100-fold with TSB, and then continuously shaken at 37 °C. OD_{600} of the bacterial suspensions were measured every hour using a microplate reader (Varioskan Flash, Thermo Fisher Scientific, Waltham, MA, USA).

2.3. Photosensitizer and laser

The photosensitizer ICG was purchased from Aladdin Industrial Corporation (Shanghai, China) and before each experiment, was dissolved in sterile PBS to a final concentration of 1024 μg/mL and stored in the dark at 4 °C A diode laser (excitation wavelength 808 nm; Mid-River Ltd., Xi'an, China) was used for PACT experiments. The distance from the laser probe to the plate surface was adjusted to obtain a power intensity of 1.5 w/cm^2. A total energy dose of 135 J/cm^2 was universally applied for all PACT experiments.

2.4. Bacterial viability assay for ICG and EDTA treatment in the dark

CFU assays were used to measure bacteria viability following treatment with ICG or EDTA in the dark. Bacterial suspensions of *S. aureus* and *P. aeruginosa* in PBS were incubated with different concentrations of ICG in the dark for 60 min at room temperature. Then, the treated bacterial suspensions were serially diluted (10-fold), and plated on Mueller-Hinton agar (MHA, Qingdao Haribo Biochemistry Instruments) plates. After incubation for 24 h at 37 °C, the CFUs were

calculated. Aliquots (100 μL) of *S. aureus* and *P. aeruginosa* suspensions in PBS were added to a 48-well plate with equal volumes of different EDTA concentrations. Then, the plates were incubated at 37 °C for 60 min. Treated bacterial suspensions were quantified *via* the colony counting methods described above.

2.5. Biofilm growth

Biofilm production by MRSA and MRPA were determined by crystal violet staining, as previously described by Barra et al. [41] with some modifications. Suspensions of both MRSA and MRPA in TSB were adjusted to a turbidity of 0.5 on the McFarland Standard, and then diluted 1:100 with TSB. Next, aliquots (200 μL) of the adjusted bacterial suspensions were transferred to a 96-well plate and incubated at 37 °C for 24 h. After the wells were aspirated and washed twice with sterile distilled water, all wells were fixed with methanol for 20 min. Biofilms were stained with 150 μL of 1% Crystal Violet solution (Beyotime Biotechnology, Shanghai, China) for 15 min, and after several washings, the wells were air dried, and then incubated with 150 μL of 95% ethanol for 20 min. Finally, the absorbance of each well at 570 nm was measured.

2.6. Photothermal effect of PACT

After 100 μL aliquots of the *S. aureus* and *P. aeruginosa* bacterial suspensions in PBS were placed in a 48-well plate with equal volumes of ICG of different concentrations, the wells were irradiated by laser at a power intensity of 1.5 w/cm^2. Temperature during irradiation was determined by an infrared camera (Fluke Ti32, Fluke Company, Everett, WA, USA).

2.7. ICG-mediated PACT on planktonic bacteria

Aliquots (100 μL) of the *S. aureus* and *P. aeruginosa* suspensions (approximately 10^7–10^8 CFU/mL) in PBS were added to a 48-well plate and divided into four groups: Control (ICG−, laser−), ICG (ICG+, laser−), Laser (ICG−, laser+), and PACT (ICG+, laser+). For the PACT group, bacterial suspensions were mixed with equal volumes of different ICG concentrations. For the ICG group, equal volumes of 128 μg/mL and 256 μg/mL ICG were mixed with *S. aureus* and *P. aeruginosa* suspensions, respectively; plates were then placed in the dark at 37 °C. For the laser and control groups, bacterial suspensions were mixed with equal volumes of PBS. After adding ICG, the wells were protected from light for 15 min, then the PACT and laser groups were irradiated for 90 s with a total light energy of 135 J/cm^2. The control group did not receive any treatment. After treatment, viable bacteria were quantified by the colony counting method described above.

2.8. The effect of EDTA combined with ICG-mediated PACT

To determine the effect of EDTA combined with ICG-mediated PACT, bacterial suspensions of *S. aureus*, MRSA, *P. aeruginosa*, and MRPA were divided into eight groups: (1) Control; (2) 2 mM EDTA alone [EDTA (2 mM)]; (3) 5 mM EDTA alone [EDTA (5 mM)]; (4) ICG and EDTA (5 mM) without irradiation [ICG + EDTA (5 mM)]; (5) Laser + EDTA (5 mM) without ICG [Laser + EDTA (5 mM)]; (6) ICG-mediated PACT (PACT-ICG); (7) ICG and EDTA (2 mM)-mediated PACT [PACT-ICG + EDTA (2 mM)]; and (8) ICG and EDTA (5 mM)-mediated PACT [PACT-ICG + EDTA (5 mM)]. Briefly, aliquots (100 μL) of suspensions of the four strains in PBS were added to a 48-well plate, then the corresponding concentrations of ICG and EDTA were added to the respective wells. Different concentrations of ICG were applied to different strains: 16 μg/mL for *S. aureus* and 64 μg/mL for *P. aeruginosa*. After a 15 min incubation with ICG and/or EDTA (as indicated), a light dose of 135 J/cm^2 was applied to the PACT and laser groups. Following each treatment, viable bacteria were determined by the colony counting method described above.

2.9. Antibacterial susceptibility assay after PACT

The antibiotic susceptibility of PACT-treated bacteria was detected by the disc diffusion (Kirby-Bauer) and microdilution methods. Suspensions of MRSA and MRPA in TSB were adjusted to a turbidity of 0.5 on the McFarland Standard, and then treated with PACT [ICG + EDTA (5 mM)] as described above. The antibiotic susceptibility was detected by the disc diffusion (Kirby-Bauer) method on MHA plates, which was conducted based on the Clinical and Laboratory Standards Institute (CLSI, 2015) MO2-A12 document [42]. The microdilution method was used to determine minimal inhibitory concentrations (MICs) of the antibiotics with some changes [43,44]. Treated and untreated suspensions were diluted with cation-adjusted Mueller-Hinton broth, and then mixed with various concentrations of antibiotics. Vancomycin (0.5, 1, 2, 4, 8, 16, and 32 μg/mL) and minocycline (0.5, 1, 2, 4, 8, 16, and 32 μg/mL) were used for MRSA, while amikacin (0.25, 0.5, 1, 2, 4, 8, and 16 μg/mL) and cefepime (1, 2, 4, 8, 16, 32, and 64 μg/mL) were used for MRPA. Mixed bacterial suspensions were incubated at 37 °C for 20 h, then MICs of PACT-treated bacteria were determined by measuring OD_{600}.

2.10. Minimum biofilm inhibitory concentration (MBIC) assay after PACT

MBICs were measured as previously described with some changes [45]. For MBIC assays of MRSA and MRPA biofilms after PACT, 400 μL of 0.5 McFarland-adjusted bacterial suspensions in TSB were placed in a 48-well plate without shaking at 37 °C for 24 h, then the plate was washed twice with sterile distilled water. The biofilms were divided into the following groups: (1) Control, (2) PACT-ICG, and (3) PACT-ICG + EDTA(5 mM). For the PACT group, the concentrations of ICG used in MRSA and MRPA were 16 μg/mL and 64 μg/mL, respectively. After PACT, biofilm bacteria were incubated with 400 μL of different vancomycin or amikacin concentrations in TSB at 37 °C for 24 h. MBICs were determined by measuring OD_{600}.

2.11. CLSM assay

For confocal studies of biofilms formed on coverslips, 2 mL of the 0.5 McFarland-adjusted bacterial suspensions in TSB were transferred into a 24-well plate with 15-mm glass coverslips and incubated at 37 °C for 24 h. Biofilms were divided into the following six groups: (1) Control; (2) EDTA; (3) Antibiotic; (4) PACT-ICG; (5) PACT-ICG + EDTA; and (6) PACT-ICG + EDTA + Antibiotics. The EDTA concentration was 5 mM in the EDTA and PACT-ICG + EDTA groups. MRSA and MRPA biofilms were treated with different antibiotics, 32 μg/mL vancomycin for MRSA, and 16 μg/mL amikacin for MRPA. After treatments, the biofilms were incubated at 37 °C for 24 h. Then, the biofilms were stained with LIVE/DEAD Baclight Bacterial Viability Kit (Molecular Probes, Eugene, OR, USA) according to the manufacturer's protocol. The kit contains two stains, a green-fluorescent SYTO9 nucleic acid stain and a red-fluorescent propidium iodide (PI) stain. SYTO9 enters all cells regardless of membrane integrity, whereas PI can only cross damaged membranes (cells with compromised membranes are usually considered dead) where it will also quench SYTO9 fluorescence. Thus, dead cells took up PI and were fluorescence red, while green fluorescent cells were considered viable. To assess bacterial viability, the two stains were simultaneously diluted in sterile water at ratios of 3:1000. After mixing, 200 μL of the solution was added to a 24-well microplate containing treated biofilms and incubated for 15 min at room temperature in the dark. After gently washing out unattached dyes, stained biofilms were observed under a Leica TCS.SP8 confocal microscope (Heidelberg, Germany). The excitation/emission wavelengths were 480/500 nm for SYTO9 and 490/635 nm for PI. Bacterial viability, the ratio of living cells relative to total cell counts, was evaluated by LAS-X

(3.3.0-16799) software.

2.12. Resazurin assay

The resazurin assay was performed to determine the metabolic activity of bacteria in biofilms after PACT and/or antibiotics treatments [46–48]. Biofilms were formed in 96-well plates and treated as for confocal imaging assays above, then 100 μL of TSB and 10 μL of Alamar Blue (Yeasen, Shanghai, China) were added to each well. After treatment, the plates were gently shaken, and then incubated in the dark for 1 h at 37 °C. Absorbance at 570 and 600 nm in the wells were determined using a microplate reader. The percent reduction in Alamar Blue staining was calculated according to the manufacturer's formula.

2.13. Statistical analysis

All statistical analyses were performed using GraphPad Prism 6.0 (GraphPad Software, La Jolla, CA, USA). All data are expressed as mean ± standard deviation. Analyses of differences between groups were performed using one-way analysis of variance, and multiple comparisons between groups were performed using Tukey's test. Results were considered statistically significant when $p < 0.05$.

3. Results

3.1. The effects of ICG and EDTA alone on bacterial viability and the photothermal effects of PACT

As shown in Fig. 1A, the four bacteria strains entered the logarithmic growth phase after 2 h. Regarding biofilm growth, the optical density at 570 nm of resolubilized Crystal Violet dye were 0.86 for MRSA and 1.07 for MRPA (Fig. 1B). ICG in the dark had no effect on the growth of the two wild-type strains, while EDTA concentration was negatively correlated with the viability of the standard strains. Compared with the control, the CFU of *P. aeruginosa* decreased by 0.48 and 1.80 (logarithmic scale) following treatment with 2 mM and 5 mM EDTA for 60 min, respectively. Regarding *S. aureus*, bacterial counts in the 2 mM and 5 mM EDTA groups decreased by 0.13 and 0.93 (logarithmic scale) respectively. Thus, there was no significant difference in CFU for the *S. aureus* 2 mM EDTA group.

Photothermal effects induced by ICG are shown in Fig. 1F. Temperatures in the 48-well plate gradually increased with ICG concentrations. At the same irradiation dose of 135 J/cm^2 with different ICG concentrations, temperatures of bacterial suspensions increased from 22.9 °C to 47.3 °C.

3.2. Inactivating planktonic bacteria with ICG-mediated PACT

As shown in Fig. 2, viable CFU counts in the *S. aureus* PACT groups were significantly reduced (Fig. 2A). There were enhanced PACT effects as ICG concentrations increased from 2 μg/mL to 16 μg/mL, while phototoxicity did not significantly increase between 16–128 μg/mL. When 16 μg/mL ICG was used, there was a 3.21 logarithmic scale reduction ($P < 0.001$), corresponding to a 99.99% efficacy.

However, viable CFU counts in the *P. aeruginosa* PACT groups were not significantly reduced (Fig. 2B). When the ICG concentration increased to 64 μg/mL, a significant reduction in the viable count following irradiation was obtained (0.39 on a logarithmic scale), corresponding to a 58.48% efficacy. Neither laser nor ICG treatment had any toxicity in *S. aureus* or *P. aeruginosa* when they were applied alone. To obtain better PACT effect and lower photothermal effect, ICG concentrations of 16 μg/mL were used for *S. aureus* and 64 μg/mL for *P. aeruginosa* in subsequent experiments.

3.3. Enhanced cytotoxicity in ICG-mediated PACT combined with EDTA treatment

For wild-type and resistant *S. aureus* strains, 2 mM EDTA had no obvious cytotoxicity, but when the concentration of EDTA increased to 5 mM, there were 0.77 and 0.42 logarithmic-scale reductions in viability, respectively (Fig. 3A). There were no significant differences in colony counts between the ICG + EDTA (5 mM) and Laser + EDTA (5 mM) groups in either strain compared with the EDTA (5 mM) group. Among the two *S. aureus* strains, there were also no differences in colony counts between the PACT-ICG and PACT-ICG + EDTA (2 mM) groups. However, compared with the PACT-ICG group, viable bacteria counts in the PACT-ICG + EDTA (5 mM) group for *S. aureus* and MRSA decreased by 1.12 and 1.92 (logarithmic scale), respectively.

For wild-type and resistant *P. aeruginosa* strains, there were no significant differences in bacterial colony counts among the EDTA, ICG + EDTA (5 mM), and Laser + EDTA (5 mM) groups, which was consistent with the *S. aureus* results (Fig. 3B). These results indicated that the laser or ICG in combination with EDTA did not increase the killing effect of EDTA. However, viable bacteria counts of the PACT-ICG + EDTA (2 mM) group were reduced by 2.01 and 1.80 (logarithmic scale) for *P. aeruginosa* and MRPA, respectively, compared with the respective PACT-ICG groups. Compared with the PACT-ICG group, viable bacteria counts in the *P. aeruginosa* and MRPA PACT-ICG + EDTA (5 mM) groups decreased by 3.65 and 4.14 (logarithmic scale), respectively. Therefore, an EDTA concentration of 5 mM was used for PACT in *S. aureus* and *P. aeruginosa* in subsequent experiments.

3.4. Enhanced antimicrobial susceptibility after PACT

The antimicrobial susceptibility after PACT treatment is in Tables 1 and 2 and Fig. 4. After PACT treatment of MRSA and MRPA, the inhibition zone of susceptible antibiotics and intermediate antibiotics increased, while that of resistant antibiotics rarely increased. After ICG + EDTA-mediated PACT treatment of MRSA, the MIC of vancomycin decreased from 1 μg/mL to 0.5 μg/mL, and the MIC of minocycline reduced from 8 μg/mL to 2 μg/mL. After ICG + EDTA-mediated PACT treatment of MRPA, the MIC of amikacin dropped from 2 μg/mL to 0.5 μg/mL, and the MIC of cefepime dropped from 16 μg/mL to 4 μg/mL. These results indicated that ICG + EDTA-mediated PACT combined with antibiotics enhanced antibiotics susceptibility.

3.5. Synergistic effects of combining ICG and EDTA-mediated PACT with antibiotics on biofilms destruction and bacterial survival

As shown in Fig. 5, the MBIC of vancomycin for MRSA in the control group was 128 μg/mL, while in the PACT-ICG and PACT-ICG + EDTA groups it was 32 μg/mL. The MBIC of amikacin for MRPA in the control and PACT-ICG groups was 64 μg/mL, while in the PACT-ICG + EDTA group it was 16 μg/mL. PACT-EDTA did

not significantly decrease MBIC compared with PACT without EDTA in MRSA biofilms. However, PACT-EDTA significantly decreased MBIC compared with PACT without EDTA in MRPA biofilms. Thus, vancomycin of 32 μg/mL was used for MRSA biofilms, and amikacin of 16 μg/mL was used for MRPA biofilms in the PACT-ICG and PACT-ICG + EDTA groups, biofilms became thinner and dead cells increased; survival ratios were 61.16% and 53.20%, respectively, compared with the controls. When biofilms treated with PACT-ICG + EDTA were dealed with vancomycin, the integrity of membrane structure was destroyed and a large number of dead cells and only a small percentage of living cells were found ; survival ratio was 12.98%. In MRPA biofilms, no obvious disruption or bacterial death were observed in the EDTA or PACT-ICG groups. When treated with amikacin alone, no biofilm disruption was observed, but bacterial survival in biofilms was reduced to 79.01%. PACT-ICG + EDTA induced more bacterial deaths than PACT-ICG. Following treatment with PACT-ICG + EDTA followed by amikacin,

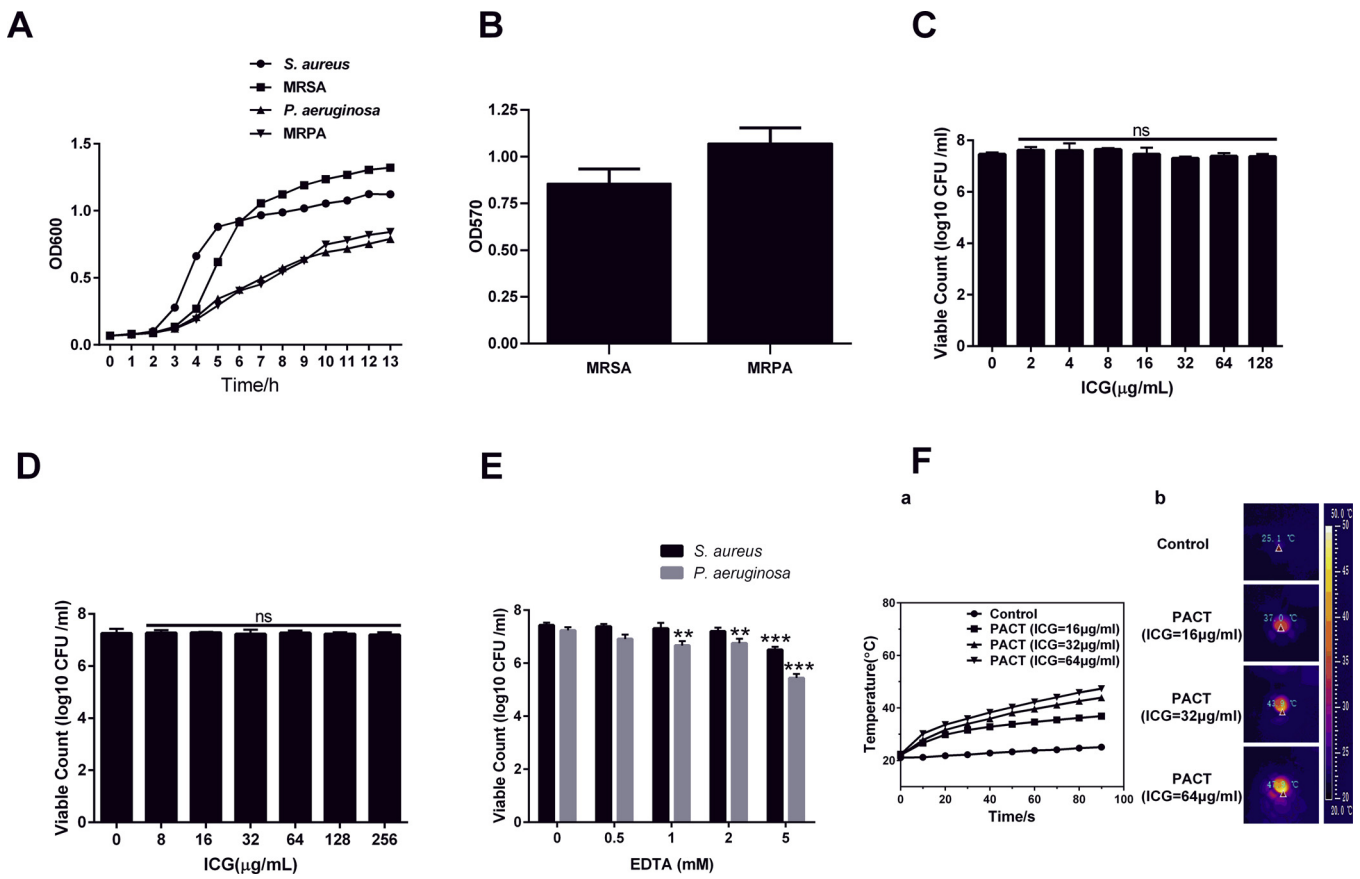

Fig. 1. The effects of ICG and EDTA alone on bacterial viability and the photothermal effects of PACT.
(A) Growth curve of four strains of bacteria. (B) Biofilm production of MRSA and MRPA. Bacterial viability for ICG in the dark on *S. aureus* (C), *P. aeruginosa* (D). (E) Effects of different concentrations of EDTA on the viability of *S. aureus* and *P. aeruginosa*. (F) a. Photothermal effect by irradiation for 90 s at a power intensity of 1.5 w/cm^2; b. Infrared imager of 48 well plates were measured at 90 seconds by irradiation. The data are shown as mean ± SD (n = 3). $^{**}P < 0.01$ and $^{***}P < 0.001$ *versus* control group. ns, no significant difference.
Abbreviation: ICG, indocyanine green; PACT, photodynamic antimicrobial chemotherapy; SD, standard deviation; MRSA, methicillin-resistant *Staphylococcus aureus*; MRPA, multidrug-resistant *Pseudomonas aeruginosa*.

biofilm detachments increased and bacterial viability decreased, it was consistent with the results of MRSA biofilms treated with PACT and vancomycin.

The metabolic activity of bacteria in biofilms was not statistically different between the EDTA and the control groups (Fig. 6D–E). Biofilms treated with vancomycin or amikacin showed a decrease in metabolic activity of 6.42% and 4.49%, respectively, compared with the controls. For MRSA biofilms, the metabolic activity of the PACT-ICG + EDTA group was 4.24% lower than that of the PACT-ICG group, but this was not statistically different. For MRPA biofilms, the metabolic activities in the PACT-ICG and PACTICG + EDTA groups were 34.66% and 16.34%, respectively, while PACT-ICG + EDTA treatment significantly reduced metabolic activity compared with the controls (33.16%). Biofilms treated with PACT-ICG + EDTA followed by antibiotic showed the lesser metabolic activity; the metabolic activities of MRSA and MRPA biofilms were 8.29% and 7.75%, respectively.

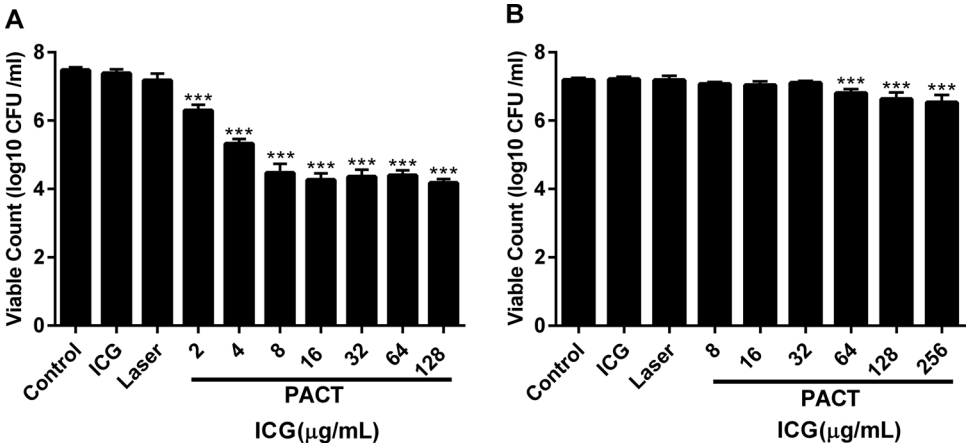

Fig. 2. Inactivation effect of ICG-mediated PACT on planktonic bacteria.
Inactivation effect of ICG mediated PACT on planktonic bacteria *S. aureus* (A), *P. aeruginosa* (B). The data are shown as mean ± SD (n = 3). $^{**}P < 0.01$ and $^{***}P < 0.001$ *versus* control group.
Abbreviation: ICG, indocyanine green; PACT, photodynamic antimicrobial chemotherapy; SD, standard deviation.

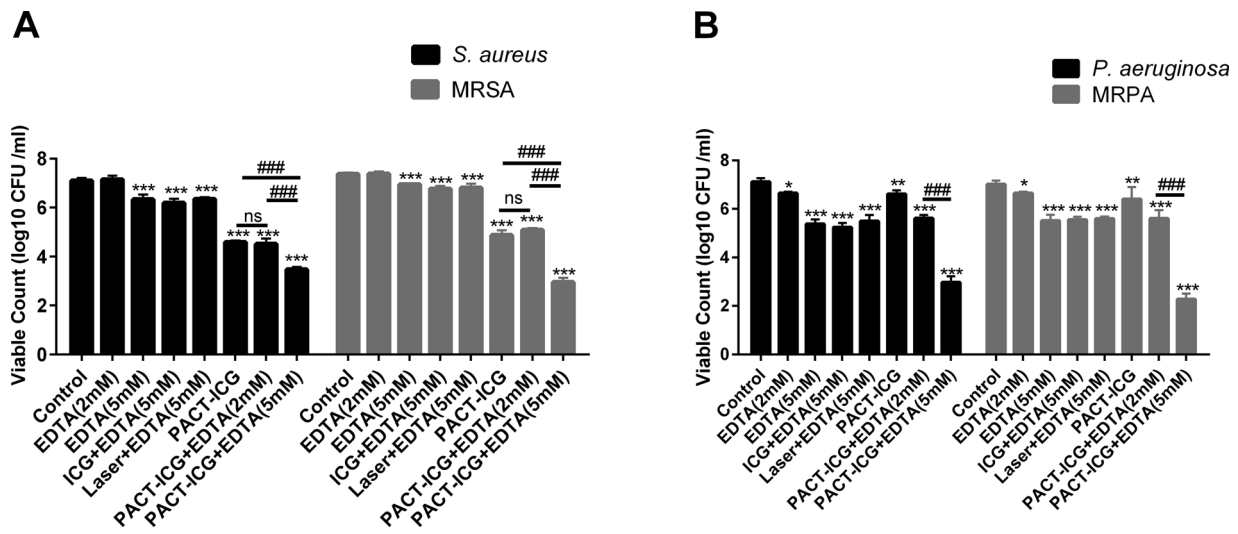

Fig. 3. Enhanced cytotoxicity in ICG-mediated PACT combined with EDTA treatment.
Enhanced cytotoxicity on *S. aureus* (A) and *P. aeruginosa* (B) in ICG-mediated PACT combined with EDTA treatment. The data are shown as mean ± SD (n = 3). $^{*}P < 0.05$, $^{**}P < 0.01$ and $^{***}P < 0.001$ *versus* control group. $^{\#\#\#}P < 0.001$ between groups. ns, no significant difference.
Abbreviation: ICG, indocyanine green; PACT, photodynamic antimicrobial chemotherapy; MRSA, methicillin-resistant *S. aureus*; MRPA, multidrug-resistant *P. aeruginosa.*

Table 1
Antimicrobial susceptibility of MRSA by disk diffusion method.

Antimicrobial Agent	Interpretive Categories and Zone Diameter Breakpoints(mm)			Antibacterial Susceptibility (mean ± SD, mm)	
	S	I	R	No treatment	PACT-ICG + EDTA
Linezolid	≥21		≤20	28.0 ± 1.0 (S)	38.0 ± 1.0 (S)
Clindamycin	≥21	15-20	≤14	28.0 ± 1.0 (S)	36.0 ± 1.0 (S)
Sulfamethoxazole	≥17	13–16	≤12	25.0 ± 1.0 (S)	31.0 ± 1.0 (S)
Gentamicin	≥15	13-14	≤12	26.0 ± 1.0 (S)	36.0 ± 2.0 (S)
Minocycline	≥19	16-18	≤15	17 ± 1.0 (I)	23.0 ± 1.0 (S)
Teicoplanin	≥19	15-18	≤14	17.0 ± 1.0 (I)	25.0 ± 1.0 (S)
Levofloxacin	≥19	16-18	≤15	6.0 ± 0.0 (R)	6.0 ± 0.0 (R)
Rifampicin	≥20	17-19	≤16	6.0 ± 0.0 (R)	6.0 ± 0.0 (R)
Penicillin	≥29		≤28	9.0 ± 1.0 (R)	12.0 ± 1.0 (R)
Erythromycin	≥23	14-22	≤13	11.5 ± 1.0 (R)	15 ± 1.0 (R)
Cefoxitin	≥22		≤21	9.0 ± 1.0(R)	11.0 ± 1.0(R)

The data are shown as mean ± SD (n = 3).
Abbreviation: S, susceptible; I, intermediate; R, resistant; ICG, indocyanine green; PACT, photodynamic antimicrobial chemotherapy; SD, standard deviation.

4. Discussion

Diabetic foot infection treatment is facing the challenge and difficulty as the emergence of antibacterial resistance and biofilm formation. We are the first to report that ICG and EDTA-mediated PACT combined with antibiotics have enhanced bactericidal effect on resistant bacterial biofilms in an *in vitro* model of DFI, making it a promising potential treatment for DFI in the future. In this study, we examined the inactivation of planktonic bacteria (wild type strains: *S. aureus* and *P. aeruginosa*) and bacteria in a biofilm (resistant strains: MRSA and MRPA) by ICG and EDTA-mediated PACT. Both ICG and EDTA have been approved by the Food and Drug Administration and are used clinically for biological and medical applications. We demonstrated that ICG-mediated PACT had a much weaker inactivation effect against *P. aeruginosa* than *S. aureus* at the same parameters, which was consistent with previous reports [27,28]. When combined with EDTA, ICG and EDTA-mediated PACT had enhanced antibacterial activity against *S. aureus* and *P. aeruginosa*, but Gram-negative *P. aeruginosa* was more sensitive to ICG and EDTA-mediated PACT than Gram-positive *S. aureus*. EDTA could improved the antibacterial effect of ICG-mediated PACT on Gram-negative bacteria, which expands the range of

Table 2
Antimicrobial susceptibility of MRPA by disk diffusion method.

Antibacterial Agent	Interpretive Categories and Zone Diameter Breakpoints (mm)			Antibacterial Susceptibility (mean ± SD, mm)	
	S	I	R	No treatment	PACT-ICG + EDTA
Amikacin	≥17	15-16	≤14	27.0 ± 2.0 (S)	34.0 ± 2.0 (S)
Ceftazidime	≥18	15-17	≤14	16.0 ± 1.0 (I)	21.0 ± 1.0 (S)
Cefepime	≥18	15-17	≤14	16.0 ± 1.0 (I)	21.0 ± 1.0 (S)
Meropenem	≥19	16-18	≤15	6.0 ± 0.0 (R)	6.0 ± 0.0 (R)
Imipenem	≥19	16-18	≤15	6.0 ± 0.0 (R)	6.0 ± 0.0 (R)
Minocycline	≥16	13-15	≤12	13.0 ± 1.0 (R)	14 ± 1.0 (R)
Ciprofloxacin	≥21	16-20	≤15	8.5 ± 1.0 (R)	14.0 ± 1.0 (R)
Levofloxacin	≥17	14-16	≤13	6.0 ± 0.0 (R)	6.0 ± 0.0 (R)
Ceftriaxone	≥21	14-20	≤13	6.0 ± 0.0 (R)	6.0 ± 0.0 (R)
Piperacillin/Tazobactam	≥21	15-20	≤14	13.0 ± 1.0 (R)	19.0 ± 1.0 (I)

The data are shown as mean ± SD (n = 3).
Abbreviation: S, susceptible; I, intermediate; R, resistant; ICG, indocyanine green; PACT, photodynamic antimicrobial chemotherapy; SD, standard deviation.

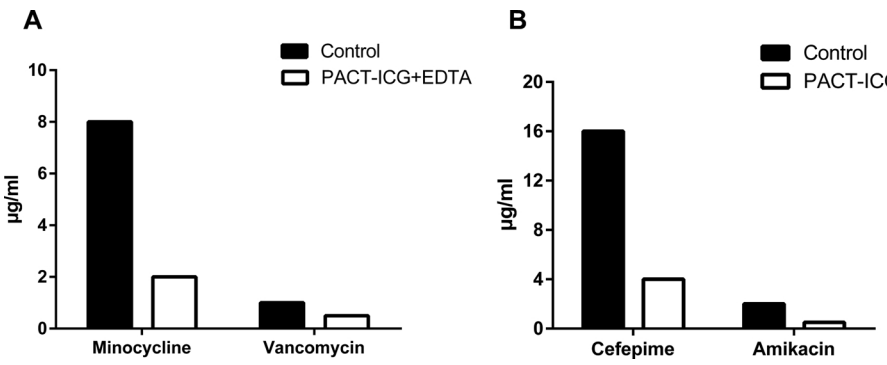

Fig. 4. The MIC of antibiotics for MRSA (A) and MRPA (B) determined by the microdilution method. The data are shown as mean ± SD (n = 3).
Abbreviation: MIC, minimum inhibitory concentration; PACT, photodynamic antibacterial chemotherapy; MRSA, methicillin-resistant *Staphylococcus aureus;* MRPA, multidrug-resistant *Pseudomonas aeruginosa*; ICG, indocyanine green; EDTA, ethylenediamine tetraacetate.

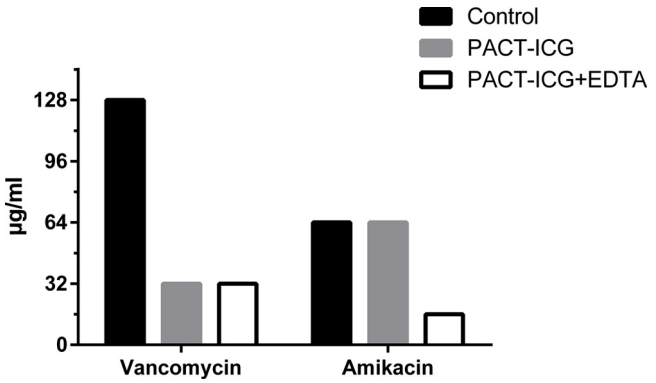

Fig. 5. Effect of ICG and/or EDTA-mediated PACT combined with antibiotics on the MBIC of MRSA and MRPA. The data are shown as mean ± SD (n = 3).
Abbreviation: MBIC, minimum biofilm inhibitory concentration; PACT, photodynamic antibacterial chemotherapy; MRSA, methicillin-resistant *Staphylococcus aureus;* MRPA, multidrug-resistant *Pseudomonas aeruginosa*; ICG, indocyanine green; EDTA, ethylenediamine tetraacetate

clinical applications for this way. Similarly, EDTA alone had only slight antibacterial effects against *S. aureus* and *P. aeruginosa*, and *P. aeruginosa* was more sensitive than *S. aureus*. This was probably due to the different outer membrane structure of Gram-positive and Gram-negative bacteria. The outer membrane surface of Gram-negative bacteria is a negatively charged quasi-continuum, and divalent cations are required to stabilize these negative charges [17]. When EDTA sequesters these cations, the stability and permeability of the outer membrane is disturbed, which facilitates uptake of the photosensitizer ICG and light penetration [17,39]. Additionally, both wild-type and drug-resistant *S. aureus* and *P. aeruginosa* strains had the same PACT effects, indicating that PACT was a nonspecific sterilization method. MBIC values, cell survival rates and the metabolic activity in biofilms all decreased by photosensitization, indicating that ICG and EDTA-mediated PACT can kill bacteria in biofilms. However, confocal imaging showed that the decreased survival of bacteria in biofilms following PACT was much lower than that observed when PACT was used against planktonic bacteria. This difference could be due to bacterial cells in a biofilm differing from their planktonic counterparts in cell wall composition, growth rate, and the presence of components in the matrix that hindered photosensitizer uptake and/or light penetration.

Along with killing planktonic and biofilm bacteria, ICG and EDTA-mediated PACT displayed a second important activity: antibacterial sensitization. We devised experiments where ICG and EDTA-mediated PACT was combined with antibiotics on planktonic and biofilms of resistant *S. aureus* and *P. aeruginosa*. We found that the combination of PACT and antibiotics was more effective than either agent alone. Notably, after PACT treatment, the inhibition zone of susceptible antibiotics and intermediate antibiotics increased for MRSA and MRPA, but that of resistant antibiotics rarely did. At the same time, the MIC of vancomycin, minocycline, amikacin, and cefepime were significantly reduced. This improvement in antibacterial susceptibility could be due to the ROS produced by PACT, which then acted on bacterial cell walls, membranes, and nucleic acids to kill bacteria and reduce colony counts [49] without altering bacterial resistance mechanisms. Therefore, the inhibitory zone of the drug-resistant antibiotics for MRSA (levofloxacin and rifampicin) did not change, nor did that of ceftriaxone, levofloxacin, imipenem, or meropenem for MRPA. Furthermore, we demonstrated that MBIC was more higher than MIC; for MRSA, the MBIC value of vancomycin was 128-fold higher than the MIC value, and for MRPA, the MBIC value of amikacin was 32-fold higher than the MIC value, which might explain why monotherapy with conventional antibiotics often fails to eradicate DFIs that include biofilms. However, when biofilms were treated with PACT, the MBIC values of MRSA and MRPA were reduced to 25% of the control. This showed that the synergistic therapy provided more antibacterial options and allowed low dose of antibiotics for clinical DFI patients.

We further tested the synergistic effects of PACT combined with antibiotics to disrupt bacterial survival and architecture in biofilms. The results from the Confocal microscopy analysis were consistent with the metabolic activity alteration in biofilm observed by Resazurin assay. Compared with other images of biofilms, only the biofilms subjected to PACT and antibiotic showed some scattered bacteria-free voids and almost all dead cells, which indicated that PACT destroyed the biofilm structure; however, the combination of PACT with antibiotics had more evident biofilm destruction. This may be due to bacterial cell membrane damage caused by PACT, which may reduce cell-to-cell contact or cell-extracellular polymeric substance (EPS) binding [50], which increases the sensitivity of bacteria to antibacterial agents. This effect might also be related to EDTA destroying the biofilm structure by chelating cations and reducing EPS crosslinking, which could increase the effects of PACT [39,51]. Additionally, we found dead cells throughout the entire thickness of PACT-treated biofilms, indicating good photosensitizer diffusion and infrared laser penetration.

In the ICG-mediated PACT on planktonic *S. aureus* testing, the CFU of viable counts did not decrease or decreased only slightly when the ICG concentration was increased from 16 μg/mL to 128 μg/mL, despite the temperatures of the bacterial suspensions increased with ICG concentration. It has been shown that decreased viable bacterial counts are primarily related to the ROS produced by PACT rather than photothermal action, which is consistent with the conclusions reported by Omar et al. [28]. Temperatures above 45 °C can induce cell necrosis, but normal tissues can tolerate this temperature due to internal heat dissipation (possibly due to augmented blood flow); even when heated to 50 °C, there is almost no damage to normal organs, tissues, or skin [52]. However, peripheral nerves and blood vessels in patients with diabetic foot ulcers may have been compromised, resulting in temperature insensitivity and poor temperature regulation. Therefore, when using ICG-mediated PACT, especially high concentration ICG, pulsed light and a cooling system is recommended to protect the skin.

This study showed that the combination of PACT and antibiotics

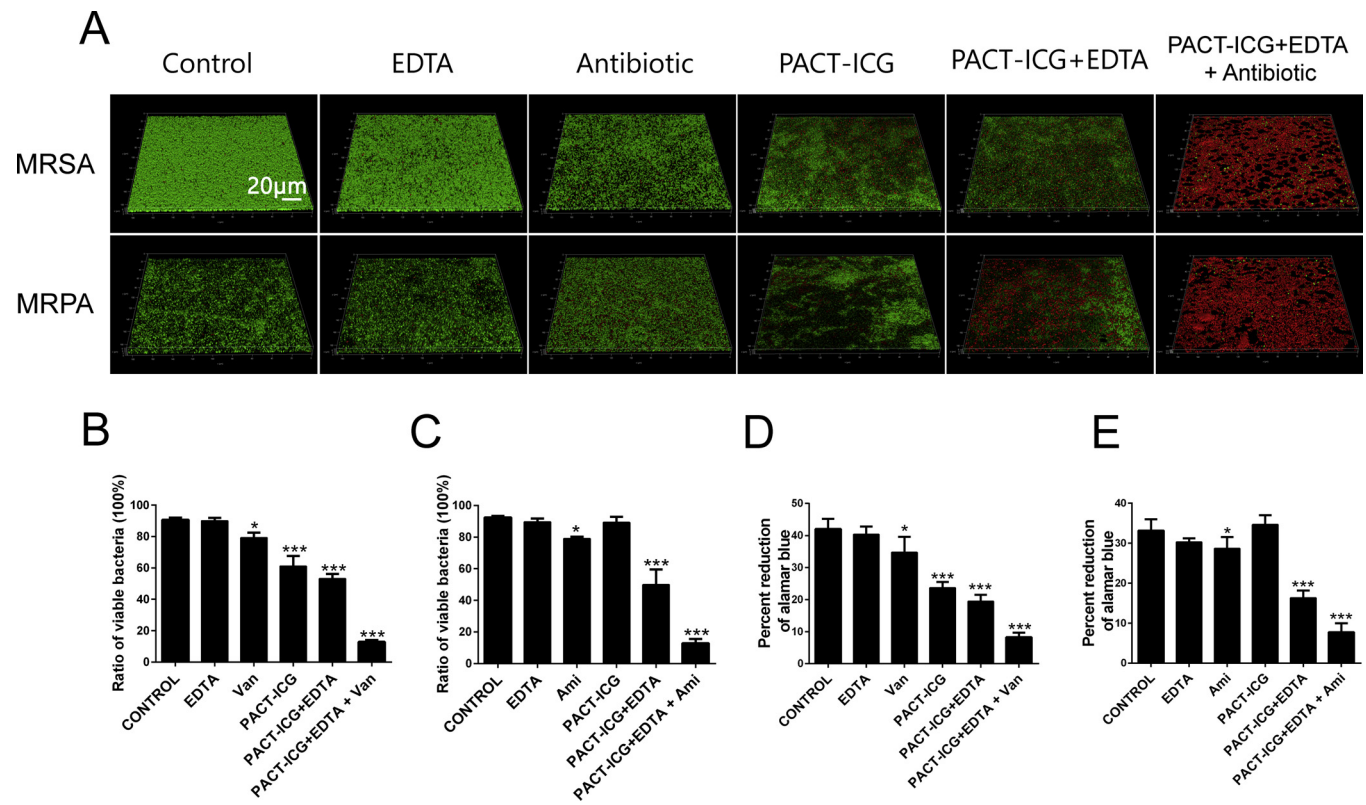

Fig. 6. Synergistic effects of combining ICG + EDTA-mediated PACT with antibiotics on biofilms destruction and bacterial survival.
(A) Three-dimensional CLSM images of biofilms disruption and bacterial survival of MRSA and MRPA with LIVE/DEAD staining. Bacterial viability of MRSA (B) and MRPA (C) were determined by LAS-X software quantitative analysis based on CLSM data. The metabolic activity of MRSA (D) and MRPA (E) biofilms were determined by Resazurin analysis. The Scale bar is 20 μm. The data are shown as mean ± SD (n = 3). $^{*}P < 0.05$, $^{**}P < 0.01$ and $^{***}P < 0.001$ *versus* the control group.
Abbreviations: CLSM, confocal laser scanning microscope; PACT, photodynamic antibacterial chemotherapy; MRSA, methicillin-resistant *Staphylococcus aureus;* MRPA, multidrug-resistant *Pseudomonas aeruginosa*; Van, vancomycin; Ami, amikacin; SD, standard deviation.

was a suitable approach to inactivate and disrupt resistant bacterial biofilms. Therefore, ICG and EDTA-mediated PACT combined with antibiotics treatment could be an interesting approach for superficial infectious diseases associated with the presence of biofilms, such as diabetic foot, burns, bedsores, dental caries, and root canal infections.

5. Conclusion

These results clearly demonstrated that the combination of EDTA and ICG-mediated PACT significantly enhanced the bactericidal effects on planktonic bacteria and resistant bacterial biofilms compared with ICG-alone-mediated PACT. The combination treatment of ICG and EDTA-mediated PACT with antibiotics successfully reduced bacterial survival in biofilms, disrupted biofilms structure and improved antibacterial susceptibility. Thus we have defined a new approach of inactivating and disrupting resistant bacterial biofilms. Therefore, this study may provide an effective and interesting approach of treating DFIs and other superficial infectious diseases with biofilms. However, this approach still needs to be clinically validated.

Disclosure statement

The authors report no conflicts of interest in this work.

Acknowledgements

This work was supported by the Basic Research and Frontier Exploration Project of the Chongqing Science and Technology Commission (Grant numbers: cstc2018jcyjAX0223 and cstc2015jcyjA10092) and the National Natural Science Foundation of China (Grant numbers: 81572558). We are very grateful to the Chongqing National Key Laboratory of Infectious Diseases and Parasites for generously gifting the bacterial strains, and the Department of Endocrinology of the First Affiliated Hospital of Chongqing Medical University for providing laser instruments.

References

[1] A. Hingorani, G.M. LaMuraglia, P. Henke, et al., The management of diabetic foot: a clinical practice guideline by the Society for Vascular Surgery in collaboration with the American Podiatric Medical Association and the Society for Vascular Medicine, J. Vasc. Surg. 63 (2 Suppl) (2016) 3S–21S.
[2] L.A. Lavery, D.G. Armstrong, D.P. Murdoch, E.J. Peters, B.A. Lipsky, Validation of the Infectious Diseases Society of America's diabetic foot infection classification system, Clin. Infect. Dis. 44 (4) (2007) 562–565.
[3] B.A. Lipsky, A.R. Berendt, P.B. Cornia, et al., Infectious Diseases Society of America clinical practice guideline for the diagnosis and treatment of diabetic foot infections, Clin. Infect. Dis. 54 (12) (2012) e132-73.
[4] K.T. Kwon, D.G. Armstrong, Microbiology and antimicrobial therapy for diabetic foot infections, Infect. Chemother. 50 (1) (2018) 11–20.
[5] R. Gadepalli, B. Dhawan, V. Sreenivas, A. Kapil, A.C. Ammini, R. Chaudhry, A clinico-microbiological study of diabetic foot ulcers in an Indian tertiary care hospital, Diabetes Care 29 (8) (2006) 1727–1732.
[6] S. Noor, A.G. Borse, M. Ozair, A. Raghav, I. Parwez, J. Ahmad, Inflammatory markers as risk factors for infection with multidrug-resistant microbes in diabetic foot subjects, Foot (Edinb) 32 (2017) 44–48.
[7] A. Hartemann-Heurtier, J. Robert, S. Jacqueminet, et al., Diabetic foot ulcer and multidrug-resistant organisms: risk factors and impact, Diabet. Med. 21 (7) (2004) 710–715.
[8] S. Pugazhendhi, A.P. Dorairaj, Appraisal of biofilm formation in diabetic foot infections by comparing phenotypic methods with the ultrastructural analysis, J. Foot Ankle Surg. 57 (2) (2018) 309–315.
[9] M. Gompelman, S.A. van Asten, E.J. Peters, Update on the role of infection and biofilms in wound healing: pathophysiology and treatment, Plast. Reconstr. Surg.

138 (3 Suppl) (2016) 61s–70s.
[10] S.L. Percival, K.E. Hill, D.W. Williams, S.J. Hooper, D.W. Thomas, J.W. Costerton, A review of the scientific evidence for biofilms in wounds, Wound Repair Regen. 20 (5) (2012) 647–657.
[11] P.S. Stewart, J.W. Costerton, Antibiotic resistance of bacteria in biofilms, Lancet 358 (9276) (2001) 135–138.
[12] C. Mottola, C.S. Matias, J.J. Mendes, et al., Susceptibility patterns of Staphylococcus aureus biofilms in diabetic foot infections, BMC Microbiol. 16 (1) (2016) 119.
[13] D.P. Nicolau, G.E. Stein, Therapeutic options for diabetic foot infections: a review with an emphasis on tissue penetration characteristics, J. Am. Podiatr. Med. Assoc. 100 (1) (2010) 52–63.
[14] T. Bjarnsholt, K. Kirketerp-Moller, P.O. Jensen, et al., Why chronic wounds will not heal: a novel hypothesis, Wound Repair Regen. 16 (1) (2008) 2–10.
[15] N. Cerca, K.K. Jefferson, R. Oliveira, G.B. Pier, J. Azeredo, Comparative antibody-mediated phagocytosis of Staphylococcus epidermidis cells grown in a biofilm or in the planktonic state, Infect. Immun. 74 (8) (2006) 4849–4855.
[16] F.F. Sperandio, Y.Y. Huang, M.R. Hamblin, Antimicrobial photodynamic therapy to kill Gram-negative bacteria, Recent Pat. Antiinfect. Drug Discov. 8 (2) (2013) 108–120.
[17] G. Jori, C. Fabris, M. Soncin, et al., Photodynamic therapy in the treatment of microbial infections: basic principles and perspective applications, Lasers Surg. Med. 38 (5) (2006) 468–481.
[18] H.Y.C. Ji Yeon Byun, Bum Myung Ki, You Won Choi, Expression of IL-10, TGF-β1 and TNF-α in Cultured Keratinocytes (HaCaT Cells) after IPL Treatment or ALA-IPL Photodynamic Treatment, Ann Dermatol (Seoul) 21 (1) (2009) 12–17.
[19] J.Y. Byun, G.Y. Lee, H.Y. Choi, K.B. Myung, Y.W. Choi, The expressions of TGF-beta (1) and IL-10 in cultured fibroblasts after ALA-IPL photodynamic treatment, Ann. Dermatol. 23 (1) (2011) 19–22.
[20] K. Sahu, M. Sharma, A. Dube, P.K. Gupta, Topical antimicrobial photodynamic therapy improves angiogenesis in wounds of diabetic mice, Lasers Med. Sci. 30 (7) (2015) 1923–1929.
[21] J.P. Tardivo, F. Adami, J.A. Correa, M.A. Pinhal, M.S. Baptista, A clinical trial testing the efficacy of PDT in preventing amputation in diabetic patients, Photodiagnosis Photodyn. Ther. 11 (3) (2014) 342–350.
[22] P.K. Lee, A. Kloser, Current methods for photodynamic therapy in the US: comparison of MAL/PDT and ALA/PDT, J. Drugs Dermatol. 12 (8) (2013) 925–930.
[23] M. Wainwright, K.B. Crossley, Methylene Blue–a therapeutic dye for all seasons? J. Chemother. 14 (5) (2002) 431–443.
[24] C. Giraudeau, A. Moussaron, A. Stallivieri, S. Mordon, C. Frochot, Indocyanine green: photosensitizer or chromophore? Still a debate, Curr. Med. Chem. 21 (16) (2014) 1871–1897.
[25] H. Abrahamse, M.R. Hamblin, New photosensitizers for photodynamic therapy, Biochem. J. 473 (4) (2016) 347–364.
[26] M.R. Detty, S.L. Gibson, S.J. Wagner, Current clinical and preclinical photosensitizers for use in photodynamic therapy, J. Med. Chem. 47 (16) (2004) 3897–3915.
[27] N. Topaloglu, M. Gulsoy, S. Yuksel, Antimicrobial photodynamic therapy of resistant bacterial strains by indocyanine green and 809-nm diode laser, Photomed. Laser Surg. 31 (4) (2013) 155–162.
[28] G.S. Omar, M. Wilson, S.P. Nair, Lethal photosensitization of wound-associated microbes using indocyanine green and near-infrared light, BMC Microbiol. 8 (111) (2008) 1–10.
[29] C. Beltes, H. Sakkas, N. Economides, C. Papadopoulou, Antimicrobial photodynamic therapy using Indocyanine green and near-infrared diode laser in reducing Entrerococcus faecalis, Photodiagnosis Photodyn. Ther. 17 (2017) (2016) 5–8.
[30] T.K. Boehm, S.G. Ciancio, Diode laser activated indocyanine green selectively kills bacteria, J. Int. Acad. Periodontol. 13 (2) (2011) 58–63.
[31] N. Topaloglu, M. Guney, S. Yuksel, M. Gulsoy, Antibacterial photodynamic therapy with 808-nm laser and indocyanine green on abrasion wound models, J. Biomed. Opt. 20 (2) (2015) 28003.
[32] V.V. Tuchin, E.A. Genina, A.N. Bashkatov, G.V. Simonenko, O.D. Odoevskaya, G.B. Altshuler, A pilot study of ICG laser therapy of acne vulgaris: photodynamic and photothermolysis treatment, Lasers Surg. Med. 33 (5) (2003) 296–310.
[33] E.A. Genina, A.N. Bashkatov, G.V. Simonenko, O.D. Odoevskaya, V.V. Tuchin, G.B. Altshuler, Low-intensity indocyanine-green laser phototherapy of acne vulgaris: pilot study, J. Biomed. Opt. 9 (4) (2004) 828–834.
[34] B.J. Kim, H.G. Lee, S.M. Woo, J.I. Youn, D.H. Suh, Pilot study on photodynamic therapy for acne using indocyanine green and diode laser, J. Dermatol. 36 (1) (2009) 17–21.
[35] M.S. Jang, K.S. Doh, J.S. Kang, Y.S. Jeon, K.S. Suh, S.T. Kim, A comparative split-face study of photodynamic therapy with indocyanine green and indole-3-acetic acid for the treatment of acne vulgaris, Br. J. Dermatol. 165 (5) (2011) 1095–1100.
[36] K. Srikanth, R.V. Chandra, A.A. Reddy, B.H. Reddy, C. Reddy, A. Naveen, Effect of a single session of antimicrobial photodynamic therapy using indocyanine green in the treatment of chronic periodontitis: a randomized controlled pilot trial, Quintessence Int. 46 (5) (2015) 391–400.
[37] M.R. Brown, R.M. Richards, Effect of ethylenediamine tetraacetate on the resistance of Pseudomonas aeruginosa to antibacterial agents, Nature 207 (5004) (1965) 1391–1393.
[38] G. Bertoloni, F. Rossi, G. Valduga, G. Jori, J. van Lier, Photosensitizing activity of water- and lipid-soluble phthalocyanines on Escherichia coli, FEMS Microbiol. Lett. 59 (1-2) (1990) 149–155.
[39] S. Finnegan, S.L. Percival, EDTA: an antimicrobial and antibiofilm agent for use in wound care, Adv. Wound Care (New Rochelle) 4 (7) (2015) 415–421.
[40] L. Leive, A nonspecific increase in permeability in escherichia coli produced by edta, Proc. Natl. Acad. Sci. U. S. A. 53 (1965) 745–750.
[41] F. Barra, E. Roscetto, A.A. Soriano, et al., Photodynamic and antibiotic therapy in combination to fight biofilms and resistant surface bacterial infections, Int. J. Mol. Sci. 16 (9) (2015) 20417–20430.
[42] CLSI, Performance standards for antibacterial disk susceptibility tests, Approved Standard 35 (1) (2015) M02–A12.
[43] M.R. Ronqui, T.M. de Aguiar Coletti, L.M. de Freitas, E.T. Miranda, C.R. Fontana, Synergistic antimicrobial effect of photodynamic therapy and ciprofloxacin, J. Photochem. Photobiol. B 158 (2016) 122–129.
[44] CLSI, Methods for dilution antibacterial susceptibility tests for bacteria that grow aerobically, Approved Standard 32 (2) (2012) M07–A9.
[45] P. Labthavikul, P.J. Petersen, P.A. Bradford, In vitro activity of tigecycline against Staphylococcus epidermidis growing in an adherent-cell biofilm model, Antimicrob. Agents Chemother. 47 (12) (2003) 3967–3969.
[46] R.K. Pettit, C.A. Weber, G.R. Pettit, Application of a high throughput Alamar blue biofilm susceptibility assay to Staphylococcus aureus biofilms, Ann. Clin. Microbiol. Antimicrob. 8 (2009) 28.
[47] H. Guo, Z. Wang, Q. Du, P. Li, Z. Wang, A. Wang, Stimulated phase-shift acoustic nanodroplets enhance vancomycin efficacy against methicillin-resistant Staphylococcus aureus biofilms, Int. J. Nanomed. 12 (2017) 4679–4690.
[48] R.K. Pettit, C.A. Weber, M.J. Kean, et al., Microplate alamar blue assay for Staphylococcus epidermidis biofilm susceptibility testing, Antimicrob. Agents Chemother. 49 (7) (2005) 2612–2617.
[49] M. Wainwright, Photodynamic antimicrobial chemotherapy (PACT), J. Antimicrob. Chemother. 42 (1) (1998) 13–28.
[50] A. Di Poto, M.S. Sbarra, G. Provenza, L. Visai, P. Speziale, The effect of photodynamic treatment combined with antibiotic action or host defence mechanisms on Staphylococcus aureus biofilms, Biomaterials 30 (18) (2009) 3158–3166.
[51] M. Sharma, L. Visai, F. Bragheri, I. Cristiani, P.K. Gupta, P. Speziale, Toluidine blue-mediated photodynamic effects on staphylococcal biofilms, Antimicrob. Agents Chemother. 52 (1) (2008) 299–305.
[52] F.K. Storm, W.H. Harrison, R.S. Elliott, D.L. Morton, Normal tissue and solid tumor effects of hyperthermia in animal models and clinical trials, Cancer Res. 39 (6 Pt. 2) (1979) 2245–2251.